
VI-PANN: HARNESSING TRANSFER LEARNING AND UNCERTAINTY-AWARE VARIATIONAL INFERENCE FOR IMPROVED GENERALIZATION IN AUDIO PATTERN RECOGNITION

A PREPRINT

John Fischer
Department of Computer Science
Naval Postgraduate School
Monterey, CA 93954
john.fischer@nps.edu

Marko Orescanin
Department of Computer Science
Naval Postgraduate School
Monterey, CA 93954
marko.orescanin@nps.edu

Eric Eckstrand
Data Science and Analytics Group
Naval Postgraduate School
Monterey, CA 93954
eric.eckstrand@nps.edu

December 14, 2023

ABSTRACT

Transfer learning (TL) is an increasingly popular approach to training deep learning (DL) models that leverages the knowledge gained by training a foundation model on diverse, large-scale datasets for use on downstream tasks where less domain- or task-specific data is available. The literature is rich with TL techniques and applications; however, the bulk of the research makes use of deterministic DL models which are often uncalibrated and lack the ability to communicate a measure of epistemic (model) uncertainty in prediction. Unlike their deterministic counterparts, Bayesian DL (BDL) models are often well-calibrated, provide access to epistemic uncertainty for a prediction, and are capable of achieving competitive predictive performance. In this study, we propose variational inference pre-trained audio neural networks (VI-PANNs). VI-PANNs are a variational inference variant of the popular ResNet-54 architecture which are pre-trained on AudioSet, a large-scale audio event detection dataset. We evaluate the quality of the resulting uncertainty when transferring knowledge from VI-PANNs to other downstream acoustic classification tasks using the ESC-50, UrbanSound8K, and DCASE2013 datasets. We demonstrate, for the first time, that it is possible to transfer calibrated uncertainty information along with knowledge from upstream tasks to enhance a model’s capability to perform downstream tasks.

Keywords audio event detection · AudioSet · Bayesian deep learning · transfer learning · uncertainty decomposition · uncertainty quantification.

1 Introduction

Transfer learning (TL) leverages knowledge gained from large foundation models to enhance performance on downstream tasks. While deterministic embeddings prevail, variational embeddings provide a promising Bayesian alternative. By using variational inference (VI) to infer posterior distributions over latent features, we obtain variational embeddings which capture uncertainty and enable new analyses of transferred representations. However, the use of variational embeddings in TL remains relatively unexplored despite their ability to capture uncertainty. Uncertainty estimation is crucial for assessing model credibility and identifying unreliable predictions [1, 2, 3, 4]. Specifically, the variance of variational embeddings provides epistemic uncertainty estimates that indicate when models lack knowledge [2, 3]. This benefits building reliable artificial intelligence systems across audio domains.

In this study, we conduct a comprehensive analysis of uncertainty-aware TL with variational audio embeddings. Bayesian versions of the popular ResNet architecture [5] are first trained on the large-scale AudioSet dataset to extract robust acoustic features along with uncertainty estimates. Building off the work of [6], we call our approach

variational inference pre-trained audio neural networks (VI-PANNs). VI-PANNs are then transferred to three audio classification benchmark datasets - ESC-50 [7], UrbanSound8K [8], and DCASE2013 [9]. Our goal is to rigorously evaluate the quality and utility of the resulting uncertainty from variational embeddings after transfer to sparse data scenarios.

While extensive work exists on uncertainty quantification and decomposition for classification problems [10, 11, 12], the focus of that work is on the multi-class case, where each sample contains only a single label. Unfortunately, this restriction hinders the application of existing techniques to real-world datasets where multiple labels may be present in each sample [13, 1, 14]. To address this limitation, we adapt the uncertainty decomposition technique from [11] and [12] for use in multi-label classifications and demonstrate its efficacy on AudioSet.

Our main contributions are: (1) we train two different VI implementations (Monte Carlo (MC) dropout [15] and Flipout [16]) of the popular ResNet-54 architecture on AudioSet and provide the checkpoints for future research; (2) we adapt the uncertainty decomposition technique from Depeweg *et al.* [11] and Chai [12] for use in multi-label classification problems; (3) we use the adapted decomposition technique to analyze the uncertainty of our pre-trained model on the AudioSet validation set; and (4) we evaluate TL with a focus on uncertainty quality using three publicly available audio datasets (ESC-50, UrbanSound8K, and DCASE2013). To our knowledge, this is the first time that the uncertainty decomposition technique from [11, 12] has been adapted for use in a multi-label classification problem.

2 Related Work

2.1 Transfer learning in audio

Recently, with popular deep learning frameworks like PyTorch offering pre-trained initializations for modern model architectures, TL has become an integral part of modern model development workflows. Building upon this, research efforts have leveraged the large-scale AudioSet dataset to pre-train deep neural networks for enhanced performance on downstream audio tasks [6, 17]. A common TL approach is to directly extract features from a pre-trained model fixed after the initial training. This method transfers general acoustic knowledge to new tasks without updating the model parameters. However, fine-tuning the pre-trained model by allowing parameter updates during training on the downstream data can further improve results by adapting to the task [6]. In this manuscript, we refer to these techniques as "fixed-feature" and "fine-tuned," respectively. Leveraging large pre-trained models via either technique provides significant performance gains across various audio applications [6, 17].

2.2 Bayesian deep learning

The inability of modern deterministic deep learning models to communicate a measure of epistemic (model) uncertainty in prediction has led to an increased interest in Bayesian deep learning (BDL), specifically in remote sensing [1, 2, 3], medical [18, 19], and safety-critical applications [20]. Although there are a number of different approaches to BDL, we focus our experiments on VI. Due to the increased speed and the ability to scale with data and models, VI is often favored over techniques like Markov Chain Monte Carlo (MCMC) [21]. In modern probabilistic machine learning libraries like BayesianTorch [22], the most common VI implementations are Flipout [16] and the Local Reparameterization Trick [23]. Due to the fact that both of these approaches represent each model weight using a Gaussian Distribution (i.e., each weight is defined using two model parameters, a mean and a variance), they effectively double the number of model parameters. In 2016, Gal *et al.* [15] showed that it was possible to perform VI by training a model with dropout layers preceding every weight layer and activating those dropout layers during inference. This approach, called MC dropout, does not double the number of model parameters. For this reason, along with the minimal changes required to common deep learning model architectures and training procedures, MC dropout is often favored over other VI approaches. In this work, we focus on the Flipout and MC dropout implementations of VI.

2.3 Uncertainty quantification and decomposition in multi-class classification

One of the primary motivations behind using BDL models is to gain access to high-quality uncertainty for predictions. The existing research literature is rich with techniques for quantifying and decomposing uncertainty. In [24], Kendall and Gal provide insight into two types of uncertainty that can be modeled. Aleatoric, or irreducible, uncertainty is the uncertainty inherent in the data. Epistemic, or reducible, uncertainty is the uncertainty about the prediction due to uncertainty about the model. In addition to providing a detailed description of these uncertainties, the authors describe a method for measuring predictive (total) uncertainty, based on output variance, and decomposing the total uncertainty into its aleatoric and epistemic components using the laws of total variance. Unfortunately, the method used by Kendall and Gal requires the use of extra parameters to model the mean and variance of the model output.

Kwon *et al.* [18] expands upon the work in [24] by proposing a method for calculating these component uncertainties without the use of additional model parameters.

Another line of research is based on the use of entropy as a measure of predictive uncertainty [11, 12]. We detail the approach of Chai [12], as we use this method for multi-class classification, and it is the basis of our multi-label classification decomposition method. In BDL multi-class classification problems, we approximate the predictive probability $p(y = c | x)$ using MC integration with M samples [25]. The average probability per class \bar{p}_c is calculated using

$$\bar{p}_c = \frac{1}{M} \sum_{m=1}^M \hat{p}_{c_m}, \quad (1)$$

where $\hat{p}_{c_m} = p(y = c | x, \theta^m)$ and θ^m is sampled from an approximation of $p(\theta | \mathcal{D})$. Defining C as the set of all possible classes, we can then compute the entropy of a prediction with

$$\mathbb{H}[y | x, \mathcal{D}] = - \sum_{c \in C} \bar{p}_c \log \bar{p}_c. \quad (2)$$

Depeweg *et al.* [11] and Chai [12] use the entropy from Eq. (2) as a measure of total uncertainty and decompose that uncertainty using the following:

$$\mathbb{H}[y | x, \mathcal{D}] = \underbrace{\mathbb{I}[y, \theta | x, \mathcal{D}]}_{\text{Epistemic}} + \underbrace{\mathbb{E}_{\theta \sim p(\theta | \mathcal{D})}[\mathbb{H}[y | x, \theta]]}_{\text{Aleatoric}}, \quad (3)$$

where \mathbb{E} is expected value and \mathbb{I} is mutual information. Similar to the calculation of predictive entropy in Eq. (2), we approximate the aleatoric uncertainty component using MC integration to arrive at the following estimator:

$$\mathbb{E}_{\theta \sim p(\theta | \mathcal{D})}[\mathbb{H}[y | x, \theta]] \approx - \frac{1}{M} \sum_{m=1}^M \sum_{c \in C} \hat{p}_{c_m} \log \hat{p}_{c_m}. \quad (4)$$

Finally, the epistemic uncertainty component is calculated by finding the difference between Eq. (2) and (4).

3 Methodology

3.1 Datasets

To comprehensively evaluate the uncertainty-aware transfer learning approach, we select a single foundation dataset, AudioSet, and three diverse audio classification datasets - ESC-50, UrbanSound8K, and DCASE2013. These datasets offer various sound recognition tasks to assess the generalization of variational embeddings. A summary of the TL dataset details is presented in Table 1.

Table 1: Description of datasets used to evaluate VI-PANN embeddings in TL

Dataset	Num Clips	Num Classes	Duration	Folds
ESC-50	2,000	50	5 sec	5
UrbanSound8K	8,732	10	≤ 4 sec	10
DCASE2013	100	10	30 sec	5

AudioSet [14]: A large-scale audio event recognition dataset consisting of 2.1M 10-second audio samples. Each of these samples were extracted from videos on YouTube and hand-annotated. Of the approximately 2.1M videos listed in the original AudioSet paper [14], we were only able to obtain approximately 1.7M (many videos from the published dataset are no longer available via the links from [14]). AudioSet has an ontology of 527 classes and is a heavily imbalanced, multi-label dataset (i.e., one or more labels can be present in a given sample). It is essential to note that the label quality varies significantly across classes, with some having noisy labels and others exhibiting high-quality annotations. Within the AudioSet data, there are three splits: a balanced evaluation split, a balanced training split, and an unbalanced training split.

ESC-50 [7]: A multi-class classification dataset which consists of 2000 five-second recordings organized into 50 classes. Split into 5-folds for cross-validation, it covers a variety of environmental sound events like gunshots, dogs barking, and applause. The ESC-50 dataset is suitable for evaluating fine-grained event recognition capabilities.

UrbanSound8K [8]: A multi-class classification dataset containing 8732 urban sound excerpts up to 4 seconds, categorized into 10 classes. Split into 10-folds for cross-validation, this dataset is commonly used to evaluate a model’s ability to identify ambient urban noises such as air conditioner, car horn, and children playing.

DCASE2013 [9]: A multi-class dataset with 10 classes representing various acoustic scenes and events. It consists of 100 audio samples, each seconds in duration, and is split into 5-folds for cross-validation. DCASE2013 is commonly used to evaluate acoustic scene/event classification in medium duration recordings.

Together, these datasets enable a rigorous evaluation of our approach on diverse audio classification tasks with labelled data far more scarce than the large foundation dataset. Furthermore, the variety of sounds and context shifts across datasets allows us to evaluate the ability of VI-PANNs to transfer and generalize their learned variational embeddings. Analyzing uncertainties on these datasets will reveal how embedding distributions capture model credibility across different acoustic environments and events.

3.2 Architecture

As a starting point, we adopt the ResNet-54 architecture described in [6] and make use of the source code provided by the authors. In order to evaluate VI-PANN, we implement MC dropout [15] and Flipout [16] variants of the pre-trained audio neural network (PANN) architecture in [6].

For the MC dropout variant, the architecture of [6] is left unmodified during training. However, during inference, we explicitly keep dropout layers active.

In order to implement the Flipout model, we utilize the Bayesian-Torch [22] software package. Using Bayesian-Torch, we convert deterministic layers to Bayesian layers. More specifically, linear layers are converted to LinearFlipout layers and Conv2d layers are converted to Conv2dFlipout. These weight layers are initialized using the MOPED methodology described in [26]. We then modify the cross entropy loss function from [6] to a loss function based on the following form of the negative Evidence Lower Bound (ELBO):

$$\mathcal{L}_q = \text{KL}[q_\phi(\theta) \parallel p(\theta)] - \mathbb{E}_q[\log p(\mathcal{D}|\theta)], \quad (5)$$

where KL corresponds to the Kullback-Leibler (KL) divergence, and \mathbb{E}_q represents the expected value under the probability distribution $q_\phi(\theta)$. A detailed discussion and derivation of this objective can be found in [2].

3.3 Uncertainty quantification and decomposition in multi-label classification

In this work, we train and evaluate BDL models on both multi-class and multi-label classification tasks. In the multi-class case (ESC-50, UrbanSound8K, and DCASE2013), we can directly apply the techniques described in Depeweg *et al.* [11] and Chai [12]. In the multi-label case (AudioSet), however, we must make a slight adaptation to account for the fact that each class is an independent binary classification problem. Following the methodology in [12], we start by calculating the predictive entropy (i.e., total uncertainty). To calculate the predictive entropy, we first calculate the entropy for each class

$$\mathbb{H}[y \mid x, \mathcal{D}] = -\bar{p}_c \log \bar{p}_c - (1 - \bar{p}_c) \log(1 - \bar{p}_c), \quad (6)$$

where \bar{p}_c is defined in Eq. (1). Next, to capture the total entropy of the prediction, we sum over all classes $\sum_{c \in C} \mathbb{H}[y \mid x, \mathcal{D}]$. Borrowing the definition of \hat{p}_{c_m} from Section 2.3, and modifying Eq. (2.21) from [12] for the multi-label case, we are left with the following estimator for aleatoric uncertainty

$$\mathbb{E}_{\theta \sim p(\theta|\mathcal{D})}[\mathbb{H}[y \mid x, \theta]] \approx - \sum_{c \in C} \frac{1}{M} \sum_{m=1}^M \hat{p}_{c_m} \log \hat{p}_{c_m} + (1 - \hat{p}_{c_m}) \log(1 - \hat{p}_{c_m}). \quad (7)$$

Finally, in order to compute epistemic uncertainty, we calculate the difference between Eq. (6) and (7),

$$\mathbb{I}[y, \theta \mid x, \mathcal{D}] \approx \mathbb{H}[y \mid x, \mathcal{D}] - \mathbb{E}_{\theta \sim p(\theta|\mathcal{D})}[\mathbb{H}[y \mid x, \theta]]. \quad (8)$$

3.4 Model evaluation

In order to align with [6] and [14], we present our pre-training results using mean average precision (mAP), area under the curve (AUC), and d-prime. Similar to [6], we calculate each metric using macro-averaging (i.e., we calculate each class individually and average across classes).

For assessing model calibration, we draw on the insights from Filos *et al.* [25], who demonstrated that a well-calibrated model’s performance improves when high-uncertainty predictions are discarded. Furthermore, Ortiz *et al.* [3, 27] demonstrated on large scale multispectral satellite datasets (multi-year data) for both classification and regression applications that proper calibration and uncertainty quantification are critical for operational use of neural network models in geoscience applications. Consequently, we employ mAP and accuracy versus data retained curves to evaluate model calibration based on predictive entropy, aleatoric uncertainty, and epistemic uncertainty. Plot shading represents a 95% confidence interval (CI) calculated over 20 replications.

To illustrate the practicality of calibrated model uncertainty, we assess each of our VI-PANNs on the ShipsEar dataset [28]. ShipsEar is a multi-class classification dataset comprising 90 underwater sound recordings of 11 different types of ships. This dataset was chosen because each sample is out-of-distribution (OOD), and the recordings, captured underwater with hydrophones, differ from the microphones used in the TL datasets in this study. Consequently, we can analyze the change in model uncertainty (total, aleatoric, and epistemic) when each model is evaluated on data types and distributions it hasn’t been trained on.

Due to the fact that our TL datasets require cross-fold validation, we present all results averaged across folds.

3.5 Bayesian deep learning model pre-training

In order to pre-train our models on AudioSet, we adopt the approach and hyper-parameters from [6]. AudioSet acoustic segments are resampled to 32kHz and converted to log-mel spectrograms using a Hamming window of 1024, a hop size of 320, and 64 mel filter banks. Additionally, we remove frequencies above 14kHz and below 50Hz from the samples. We use a batch size of 32, and an Adam optimizer with a learning rate of 0.001. For the MC dropout variants, we use a dropout rate of 0.2 for convolutional layers, and 0.5 for linear layers.

We apply this training setup to our YouTube-curated repository of approximately 1.7M 10-second, unbalanced audio clips. Similar to [6], we employ mixup [29] augmentation with $\alpha = 1.0$; however, we make no effort to balance the training dataset. As the goal of our investigation is not to match state-of-the-art performance on the AudioSet tagging task but rather construct large-parameter probabilistic versions of AudioSet pre-trained networks to investigate the benefits they confer to uncertainty analysis in the acoustic domain, we train our deterministic PANN and MC dropout VI-PANN for approximately 3M steps. In order to train our Flipout VI-PANN, we initialize the network priors and posteriors using MOPED [26] with the learned weights from our deterministic PANN. We then train the Flipout VI-PANN for an additional 2M steps. The deterministic PANN and both VI-PANNs are evaluated using the AudioSet balanced evaluation split.

3.6 Bayesian transfer learning

In our TL experiments, we explore three distinct TL strategies.

1. Flip Strategy:

- Initialize a Flipout model with parameters from our Flipout VI-PANN.
- Replace the classification head with a new Flipout head, using the Bayesian-Torch LinearFlipout layer defaults.
- Freeze the backbone, train the classification head for 200 epochs with a learning rate of 0.001 (referred to as "fixed-feature"), then unfreeze the backbone, reduce the learning rate by a factor of 10, and train for an additional 200 epochs (referred to as "fine-tuned").

2. Det-Flip Strategy:

- Initialize a deterministic model with our deterministic PANN using MOPED.
- Replace the deterministic head with a Flipout head, following the Flip strategy workflow.

3. Drop Strategy:

- Initialize an MC dropout model with our MC dropout VI-PANN.

- Replace the head with an MC dropout head (dropout rate: 0.5), and follow the Flip strategy workflow.

For comparison, we include results from a deterministic baseline (**Det**):

- Initialize a deterministic model with our deterministic PANN.
- Replace the head with a deterministic head and follow the Flip strategy training workflow.

These diverse strategies allow us to assess the impact of different transfer learning approaches on model performance.

4 Results and Discussion

4.1 Foundation model (AudioSet)

The results of our AudioSet pre-training are summarized in Table 2. Each of our models exhibits comparable performance, as measured by mAP, AUC, and d-prime, to the ResNet-54 PANN presented in [6]. Alongside performance metrics, we provide predictive entropy (total uncertainty), epistemic uncertainty, and aleatoric uncertainty calibration plots for our VI-PANNs in Fig. 1.

Table 2: AudioSet Pre-Training Results

Model	mAP	AUC	d-prime
Det	0.418	0.973	2.732
Drop	0.426	0.975	2.762
Flip	0.415	0.972	2.708
ResNet-54 PANN [6]	0.429	0.971	2.675

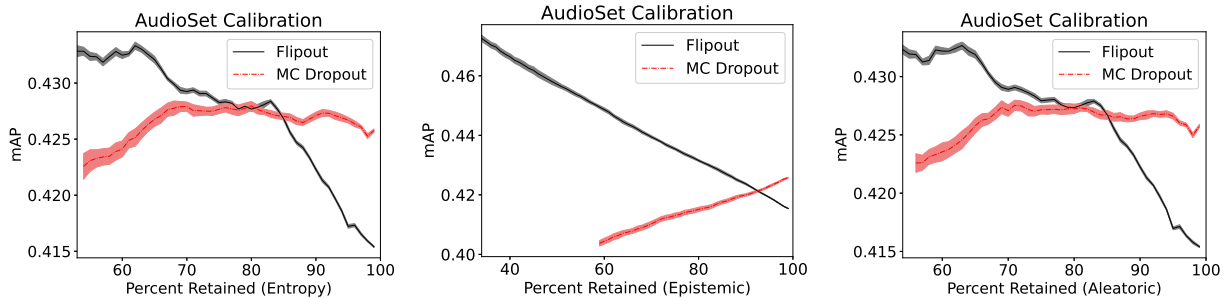


Figure 1: Uncertainty calibration plots for foundation model training on AudioSet. Comparison plot of test set accuracy vs. percentage of evaluation data retained based on entropy (left), epistemic uncertainty (center), and aleatoric uncertainty (right). Shading represents a 95% CI.

Our Flipout VI-PANN demonstrates well-calibrated uncertainty across all three measures. In contrast, the MC dropout VI-PANN exhibits poor calibration. A well-calibrated model typically shows improved performance as high-uncertainty predictions are discarded [25]. The observed poor calibration is likely attributed to the complexity and significant class imbalance within the AudioSet dataset. Additionally, the lack of explicit learning of the dropout parameter during the training process may contribute to this issue [30].

In Fig. 2, we present box plots that compare the model uncertainty on both the AudioSet test set and the ShipsEar dataset. Although results from both the Flipout and MC Dropout models are included, our primary focus is on the Flipout model due to its demonstrated calibration across all three types of uncertainty. Upon analyzing the model’s response to samples from the ShipsEar dataset, we observe a subtle increase in both average entropy and aleatoric uncertainty when compared to the AudioSet test set. Conversely, the average epistemic uncertainty remains consistent across both datasets. Notably, the plots reveal a tighter distribution of uncertainty on the ShipsEar dataset in contrast to the AudioSet dataset. This phenomenon is likely attributed to the diversity of the input data, extreme class imbalance, and unsatisfactory label quality observed in many underrepresented classes within the AudioSet dataset.

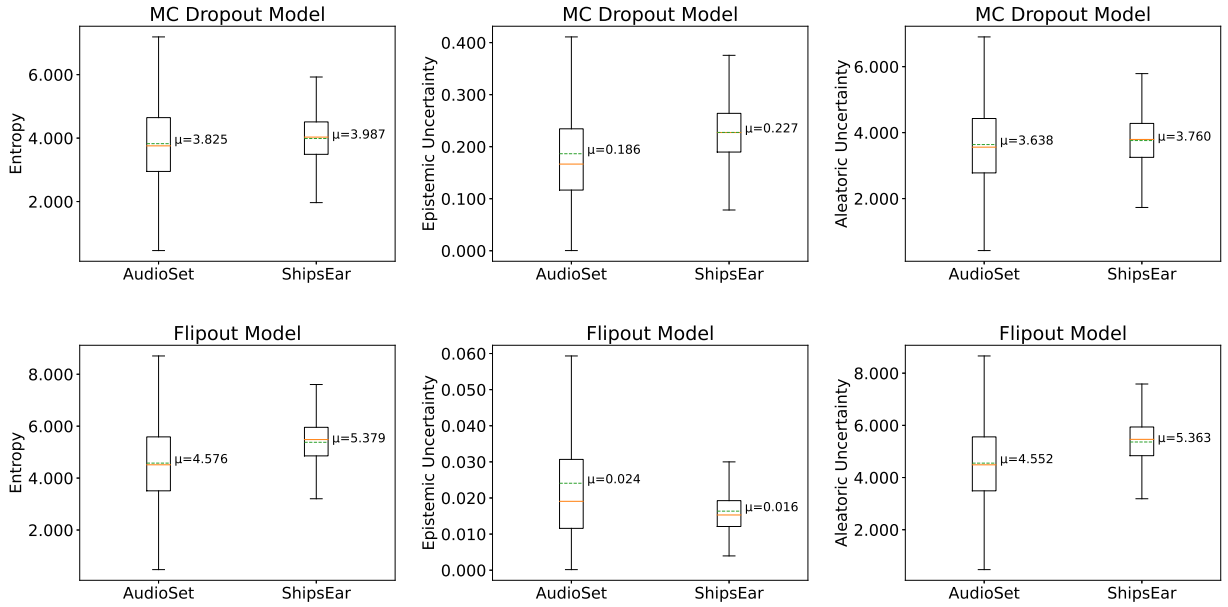


Figure 2: Uncertainty box plots depicting results of MC Dropout model (top row) and Flipout model (bottom row) trained on AudioSet. The plots compare predictive entropy (left), epistemic uncertainty (middle), and aleatoric uncertainty (right) as the models are evaluated on both the AudioSet test set and the ShipsEar dataset. Both the median (orange line) and mean (dashed green line) are presented.

4.2 Transfer Learning

The transfer learning (TL) results for ESC-50, UrbanSound8K, and DCASE2013 are detailed in Table 3. For context, the results of training models from scratch (i.e., without TL) are also provided in Table 4. Each model variant (Det, Det-Flip, Drop, Flip) exhibits comparable performance across the three datasets. Notably, fine-tuned models demonstrate a substantial increase in accuracy compared to fixed-feature (fixed) models and both TL techniques provide significant performance increases over the models trained from scratch on the TL datasets. As expected, when trained from scratch on the relatively small TL datasets, the high-capacity ResNet-54 models perform relatively poorly and suffer from overfitting. The Flip variant which contains 2x the learnable parameters, when compared to the other variants, performs particularly poorly. Although the Det PANN slightly outperforms others in accuracy on ESC-50 and DCASE2013, it lacks the capability to provide access to epistemic uncertainty in predictions.

Table 3: Transfer Learning Results (Accuracy)

Model	ESC-50		UrbanSound8K		DCASE2013	
	Fixed	Fine-Tuned	Fixed	Fine-Tuned	Fixed	Fine-Tuned
Flip	0.934	0.950	0.857	0.873	0.860	0.870
Det-Flip	0.951	0.962	0.858	0.874	0.790	0.850
Drop	0.952	0.958	0.864	0.873	0.830	0.860
Det	0.951	0.964	0.858	0.870	0.870	0.880

Table 4: Baseline Model Performance (Accuracy)–Training Without TL

Model	ESC-50	UrbanSound8k	DCASE2013
Flip	0.422	0.794	0.400
Det-Flip	0.834	0.815	0.610
Drop	0.861	0.827	0.680
Det	0.858	0.827	0.730

Furthermore, we provide calibration plots for UrbanSound8K (Figs. 3 and 4), ESC-50 (Figs. 6 and 7), and DCASE2013 (Figs. 9 and 10). These plots reveal that, following TL, when fixing the features of the base model and after fine-tuning, all three variants of our VI-PANNs result in well-calibrated models. The staircase pattern evident in the DCASE2013 plots is attributed to the comparatively small size of the DCASE2013 dataset.

In each of the UrbanSound8k calibration plots, the curve of the TL model learned from fixed-features starts at a lower accuracy and crosses over that of the TL model fine-tuned, achieving a higher accuracy at the same percentage of data retained. These results suggest that fine-tuning may have an adverse effect on model calibration if care is not taken in the fine-tuning process. Intuitively, one might extend the hyperparameter evaluation of fine-tuning and model selection to include calibration curve.

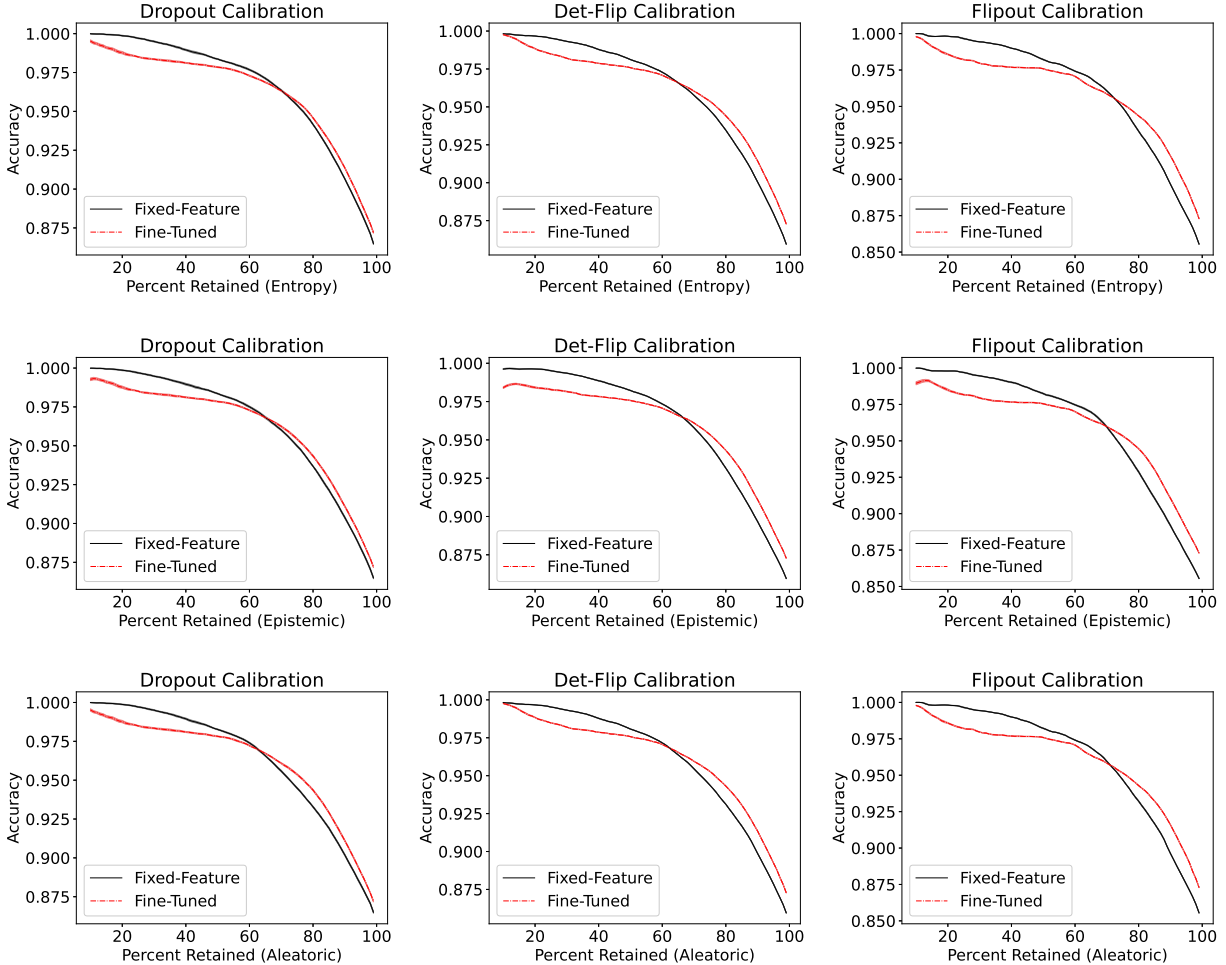


Figure 3: Uncertainty calibration plots comparing fixed-feature and fine-tuning TL techniques on UrbanSound8K. Comparison plots of test set accuracy vs. percentage of evaluation data retained based on Entropy (top), Epistemic Uncertainty (middle) and Aleatoric Uncertainty (bottom). Drop VI-PANN is on the left, Det-Flip VI-PANN in the center, and Flip VI-PANN on the right. Shading represents a 95% CI.

In Figs. 5, 8, and 11, we depict box plots that compare model uncertainty for each of the TL datasets (UrbanSound8k, ESC-50, and DCASE2013) and the ShipsEar dataset. Since the fine-tuned models demonstrated superior performance compared to the fixed-feature models, we showcase the results of the fine-tuned Dropout, Flipout, and Det-Flip models. In contrast to the AudioSet results, when assessed on the ShipsEar dataset, all three model variants exhibit a notable increase in average entropy, epistemic uncertainty, and aleatoric uncertainty compared to the TL dataset. Moreover, the plots illustrate a considerably broader distribution of uncertainty compared to the TL datasets. This outcome is anticipated given that these models perform exceptionally well with low uncertainty on the TL datasets.

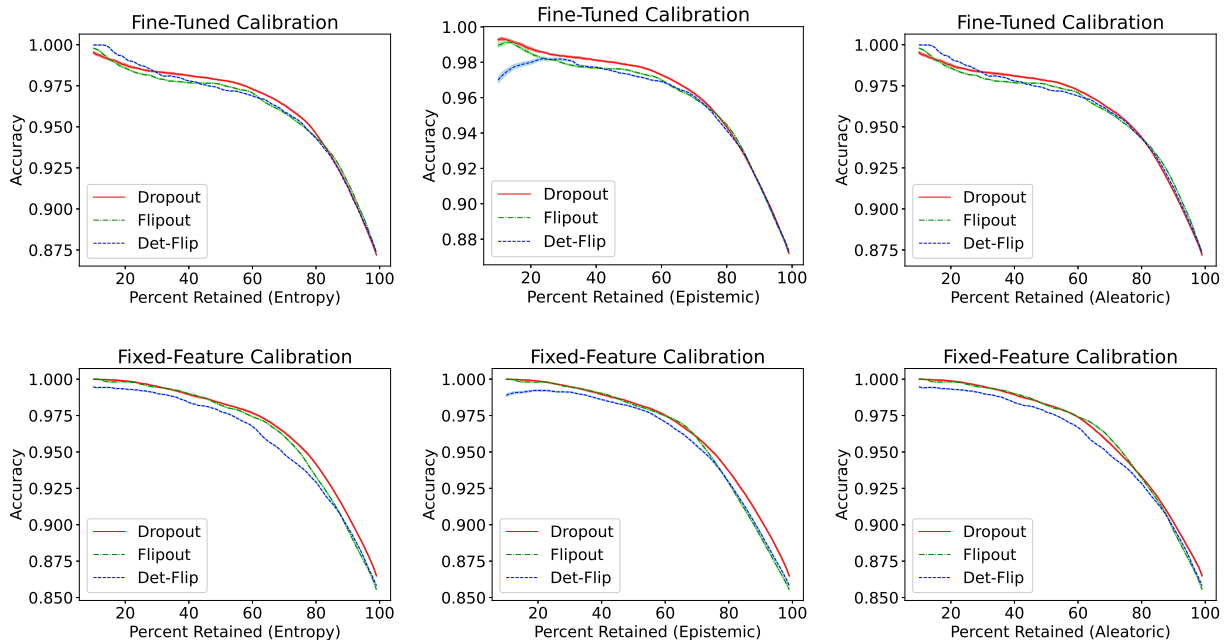


Figure 4: Uncertainty calibration plots comparing Drop, Flip, and Det-Flip VI-PANN variants on UrbanSound8k. Comparison plots of test set accuracy vs. percentage of evaluation data retained based on Entropy (left), Epistemic Uncertainty (center) and Aleatoric Uncertainty (right). Plots corresponding to fine-tuned models are on the top, fixed-feature model plots are on the bottom. Shading represents a 95% CI.

5 Conclusion

In this study, we introduce VI-PANNs as a Bayesian alternative to widely adopted deterministic audio embedding methods. Trained on AudioSet, our VI-PANNs exhibit calibrated models through the use of the Flipout approach, underscoring the significance of variational audio embeddings. By adapting uncertainty decomposition techniques for multi-label classification, we enable a nuanced analysis of uncertainty estimates not only on AudioSet but also on other multi-label datasets. Notably, our work represents the first adaptation of the uncertainty decomposition from [11, 12] for application in multi-label problems.

Our transfer learning (TL) experiments on well-established datasets demonstrate comparable or improved performance compared to previous state-of-the-art methods, leveraging a similar model architecture. Importantly, our Det-Flip VI-PANN, constructed with a deterministic PANN and a Flipout classification head, achieves high performance at a relatively low cost compared to pre-training a full Flipout model. This establishes robust baselines for uncertainty-aware audio transfer learning in scenarios with limited labeled data, offering valuable insights for practitioners.

Crucially, the presented methodology for TL with variational audio embeddings is universal and applicable to diverse audio tasks. The insights gained emphasize the intrinsic value of Bayesian neural networks in facilitating reliable and transparent transfer learning within the audio domain.

6 Disclaimer

The views and conclusions contained herein are those of the authors and should not be interpreted as necessarily representing the official policies or endorsements, either expressed or implied, of the U.S. Government. The U.S. Government is authorized to reproduce and distribute reprints for Government purposes notwithstanding any copyright annotations thereon.

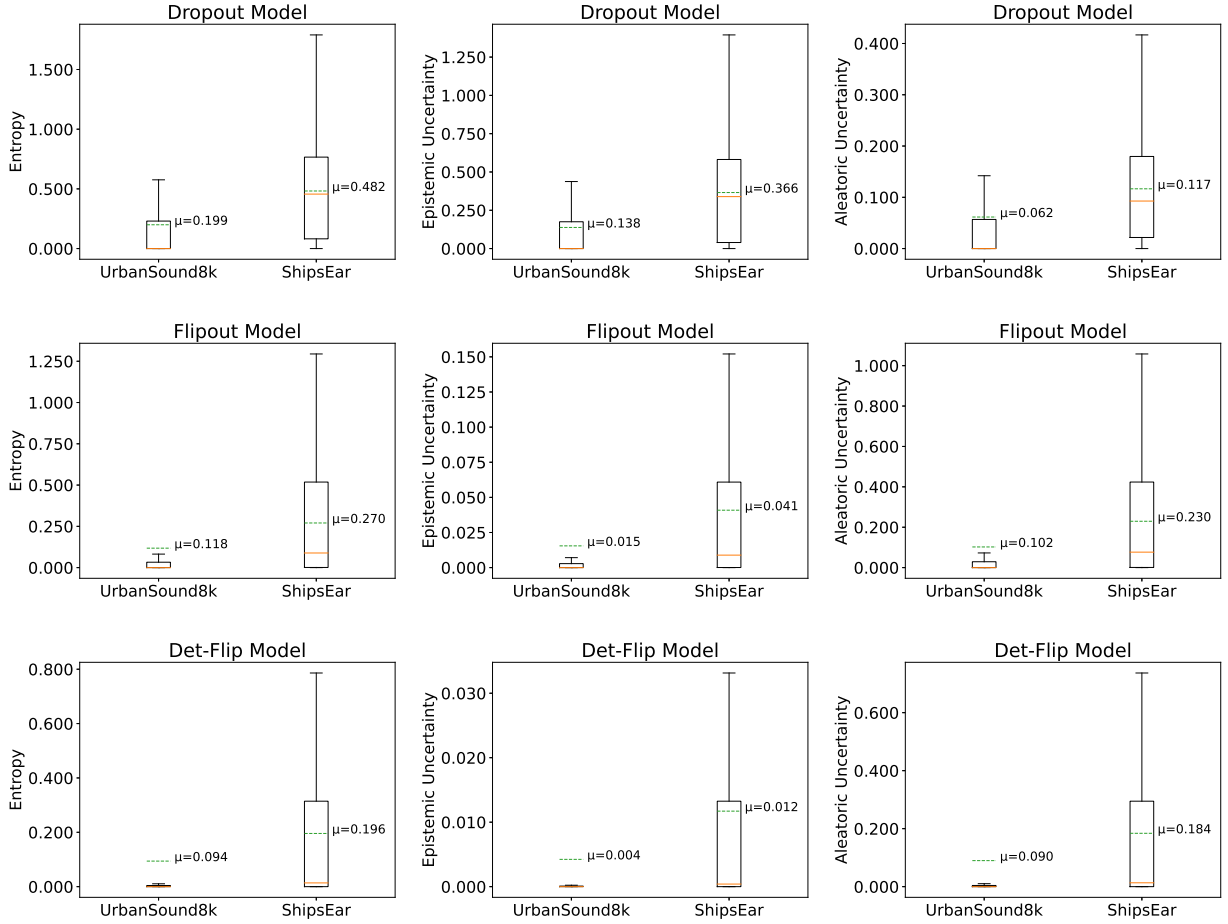


Figure 5: Uncertainty box plots depicting results of MC Dropout (top row), Flipout (middle row), and Det-Flip (bottom row) fine tuned on UrbanSound8k. The plots compare predictive entropy (left), epistemic uncertainty (middle), and aleatoric uncertainty (right) as the models are evaluated on both UrbanSound8k and the ShipsEar dataset. Both the median (orange line) and mean (dashed green line) are presented.

References

- [1] Brandon Beckler, Andrew Pfau, Marko Orescanin, Sabrina Atchley, Nicholas Villemez, John E. Joseph, Christopher W. Miller, and Tetyana Margolina, “Multilabel classification of heterogeneous underwater soundscapes with Bayesian deep learning,” *IEEE Journal of Oceanic Engineering*, vol. 47, no. 4, pp. 1143–1154, 2022.
- [2] John Fischer, Marko Orescanin, Paul Leary, and Kevin B. Smith, “Active Bayesian deep learning with vector sensor for passive sonar sensing of the ocean,” *IEEE Journal of Oceanic Engineering*, vol. 48, no. 3, pp. 837–852, 2023.
- [3] Pedro Ortiz, Marko Orescanin, Veljko Petković, Scott W. Powell, and Benjamin Marsh, “Decomposing satellite-based classification uncertainties in large earth science datasets,” *IEEE Transactions on Geoscience and Remote Sensing*, vol. 60, pp. 1–11, 2022.
- [4] Marko Orescanin, Veljko Petković, Scott W Powell, Benjamin R Marsh, and Sean C Heslin, “Bayesian deep learning for passive microwave precipitation type detection,” *IEEE Geoscience and Remote Sensing Letters*, 2021.
- [5] Kaiming He, Xiangyu Zhang, Shaoqing Ren, and Jian Sun, “Deep residual learning for image recognition,” in *Proceedings of the IEEE conference on computer vision and pattern recognition*, 2016, pp. 770–778.
- [6] Qiuqiang Kong, Yin Cao, Turab Iqbal, Yuxuan Wang, Wenwu Wang, and Mark D. Plumbley, “PANNs: Large-scale pretrained audio neural networks for audio pattern recognition,” *IEEE/ACM Transactions on Audio, Speech, and Language Processing*, vol. 28, pp. 2880–2894, 2020.

- [7] Karol J. Piczak, “ESC: Dataset for Environmental Sound Classification,” in *Proceedings of the 23rd Annual ACM Conference on Multimedia*. 2015, pp. 1015–1018, ACM Press.
- [8] Justin Salamon, Christopher Jacoby, and Juan Pablo Bello, “A dataset and taxonomy for urban sound research,” in *Proceedings of the 22nd ACM International Conference on Multimedia*, New York, NY, USA, 2014, MM ’14, p. 1041–1044, Association for Computing Machinery.
- [9] Dan Stowell, Dimitrios Giannoulis, Emmanouil Benetos, Mathieu Lagrange, and Mark D. Plumbley, “Detection and classification of acoustic scenes and events,” *IEEE Transactions on Multimedia*, vol. 17, no. 10, pp. 1733–1746, 2015.
- [10] Yarin Gal, *Uncertainty in Deep Learning*, Ph.D. thesis, University of Cambridge, 2016.
- [11] Stefan Depeweg, Jose-Miguel Hernandez-Lobato, Finale Doshi-Velez, and Steffen Udfluft, “Decomposition of uncertainty in Bayesian deep learning for efficient and risk-sensitive learning,” in *Proceedings of the 35th International Conference on Machine Learning*, Jennifer Dy and Andreas Krause, Eds. 10–15 Jul 2018, vol. 80 of *Proceedings of Machine Learning Research*, pp. 1184–1193, PMLR.
- [12] Lucy R Chai, *Uncertainty estimation in Bayesian neural networks and links to interpretability*, M.S. thesis, University of Cambridge, 2018.
- [13] Andrew M. Pfau, “Multi-label classification of underwater soundscapes using deep convolutional neural networks,” M.S. thesis, Naval Postgraduate School, Monterey, CA, 2020.
- [14] Jort F. Gemmeke, Daniel P. W. Ellis, Dylan Freedman, Aren Jansen, Wade Lawrence, R. Channing Moore, Manoj Plakal, and Marvin Ritter, “Audio set: An ontology and human-labeled dataset for audio events,” in *Proc. IEEE ICASSP 2017*, New Orleans, LA, 2017.
- [15] Yarin Gal and Zoubin Ghahramani, “Dropout as a Bayesian approximation: Representing model uncertainty in deep learning,” in *international conference on machine learning*. PMLR, 2016, pp. 1050–1059.
- [16] Yeming Wen, Paul Vicol, Jimmy Ba, Dustin Tran, and Roger B. Grosse, “Flipout: Efficient pseudo-independent weight perturbations on mini-batches,” in *6th International Conference on Learning Representations, ICLR 2018, Vancouver, BC, Canada, April 30 - May 3, 2018, Conference Track Proceedings*. 2018, OpenReview.net.
- [17] Paulo Lopez-Meyer, Juan A. del Hoyo Ontiveros, Hong Lu, and Georg Stemmer, “Efficient end-to-end audio embeddings generation for audio classification on target applications,” in *ICASSP 2021 - 2021 IEEE International Conference on Acoustics, Speech and Signal Processing (ICASSP)*, 2021, pp. 601–605.
- [18] Yongchan Kwon, Joong-Ho Won, Beom Joon Kim, and Myunghee Cho Paik, “Uncertainty quantification using Bayesian neural networks in classification: Application to biomedical image segmentation,” *Computational Statistics & Data Analysis*, vol. 142, pp. 106816, 2020.
- [19] Patrick McClure, Charles Y. Zheng, Jakub Kacmarzyk, John Rogers-Lee, Satrajit S. Ghosh, Dylan Nielson, Peter A. Bandettini, and Francisco Pereira, “Distributed weight consolidation: A brain segmentation case study,” in *Advances in Neural Information Processing Systems 31: Annual Conference on Neural Information Processing Systems 2018, NeurIPS 2018, December 3-8, 2018, Montréal, Canada*, Samy Bengio, Hanna M. Wallach, Hugo Larochelle, Kristen Grauman, Nicolò Cesa-Bianchi, and Roman Garnett, Eds., 2018, pp. 4097–4107.
- [20] Fabio Arnez, Huascar Espinoza, Ansgar Radermacher, and François Terrier, “Towards dependable autonomous systems based on bayesian deep learning components,” in *2022 18th European Dependable Computing Conference (EDCC)*, 2022, pp. 65–72.
- [21] Matthew D. Hoffman, David M. Blei, Chong Wang, and John Paisley, “Stochastic variational inference,” *Journal of Machine Learning Research*, vol. 14, no. 4, pp. 1303–1347, 2013.
- [22] Ranganath Krishnan, Pi Esposito, and Mahesh Subedar, “Bayesian-torch: Bayesian neural network layers for uncertainty estimation,” <https://github.com/IntelLabs/bayesian-torch>, Jan. 2022.
- [23] Durk P Kingma, Tim Salimans, and Max Welling, “Variational dropout and the local reparameterization trick,” in *Advances in Neural Information Processing Systems*, C. Cortes, N. Lawrence, D. Lee, M. Sugiyama, and R. Garnett, Eds. 2015, vol. 28, Curran Associates, Inc.
- [24] Alex Kendall and Yarin Gal, “What uncertainties do we need in Bayesian deep learning for computer vision?,” in *Advances in Neural Information Processing Systems*, I. Guyon, U. V. Luxburg, S. Bengio, H. Wallach, R. Fergus, S. Vishwanathan, and R. Garnett, Eds. 2017, vol. 30, Curran Associates, Inc.
- [25] Angelos Filos, Sebastian Farquhar, Aidan N Gomez, Tim GJ Rudner, Zachary Kenton, Lewis Smith, Milad Alizadeh, Arnoud de Kroon, and Yarin Gal, “A systematic comparison of Bayesian deep learning robustness in diabetic retinopathy tasks,” *arXiv preprint arXiv:1912.10481*, 2019.

- [26] Ranganath Krishnan, Mahesh Subedar, and Omesh Tickoo, “Specifying weight priors in Bayesian deep neural networks with empirical Bayes,” in *Proceedings of the AAAI Conference on Artificial Intelligence*, 2020, vol. 34, pp. 4477–4484.
- [27] Pedro Ortiz, Eleanor Casas, Marko Orescanin, Scott W. Powell, Veljko Petkovic, and Micky Hall, “Uncertainty calibration of passive microwave brightness temperatures predicted by bayesian deep learning models,” *Artificial Intelligence for the Earth Systems*, vol. 2, no. 4, pp. e220056, 2023.
- [28] David Santos-Domínguez, Soledad Torres-Guijarro, Antonio Cardenal-López, and Antonio Pena-Gimenez, “ShipsEar: An underwater vessel noise database,” *Applied Acoustics*, vol. 113, pp. 64–69, Dec. 2016.
- [29] Hongyi Zhang, Moustapha Cisse, Yann N. Dauphin, and David Lopez-Paz, “mixup: Beyond empirical risk minimization,” in *International Conference on Learning Representations*, 2018.
- [30] Yarin Gal, Jiri Hron, and Alex Kendall, “Concrete dropout,” in *Neural Information Processing Systems*, 2017.

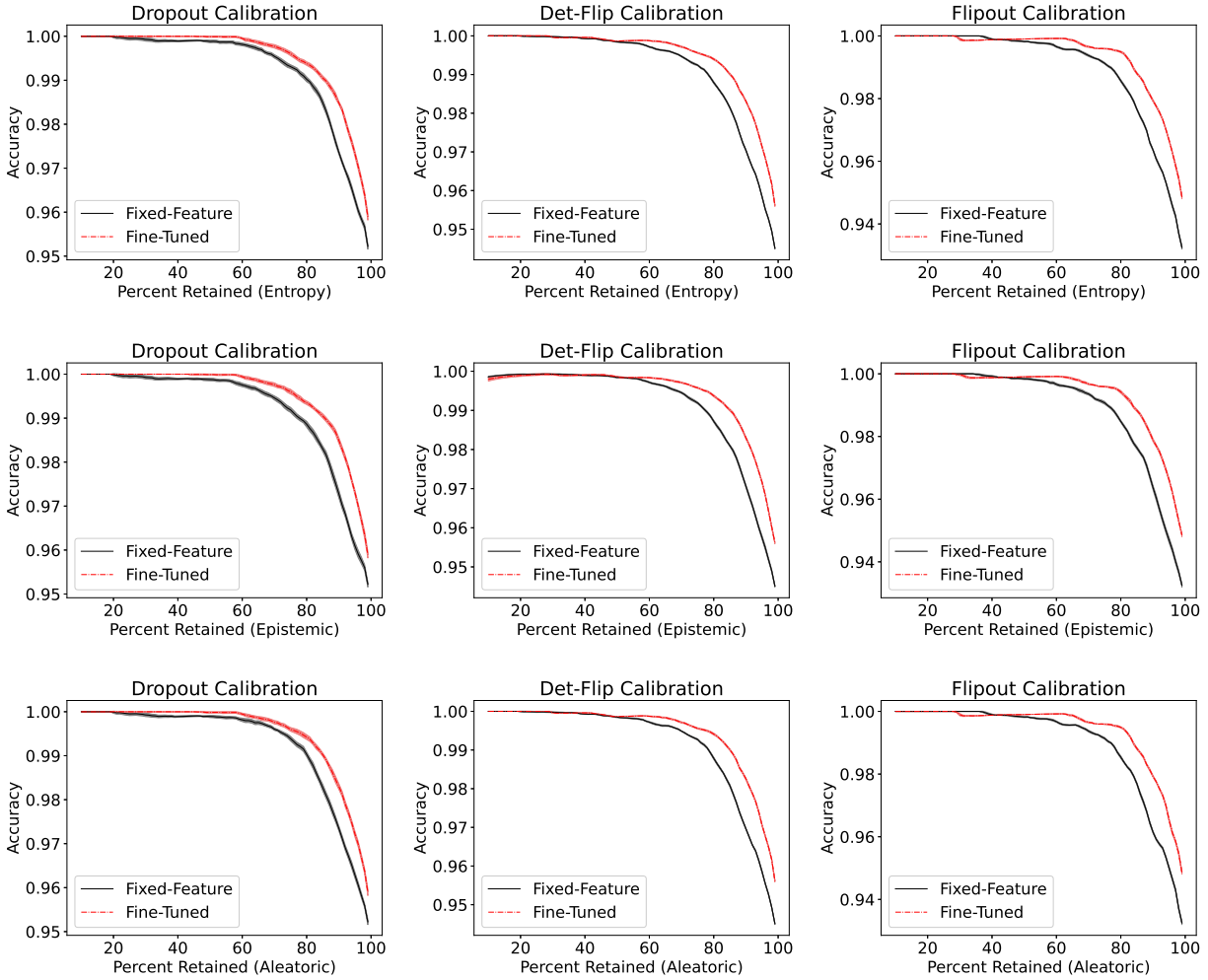


Figure 6: Uncertainty calibration plots comparing fixed-feature and fine-tuning TL techniques on ESC-50. Comparison plots of test set accuracy vs. percentage of evaluation data retained based on Entropy (top), Epistemic Uncertainty (middle) and Aleatoric Uncertainty (bottom). Drop VI-PANN is on the left, Det-Flip VI-PANN in the center, and Flip VI-PANN on the right. Shading represents a 95% CI.

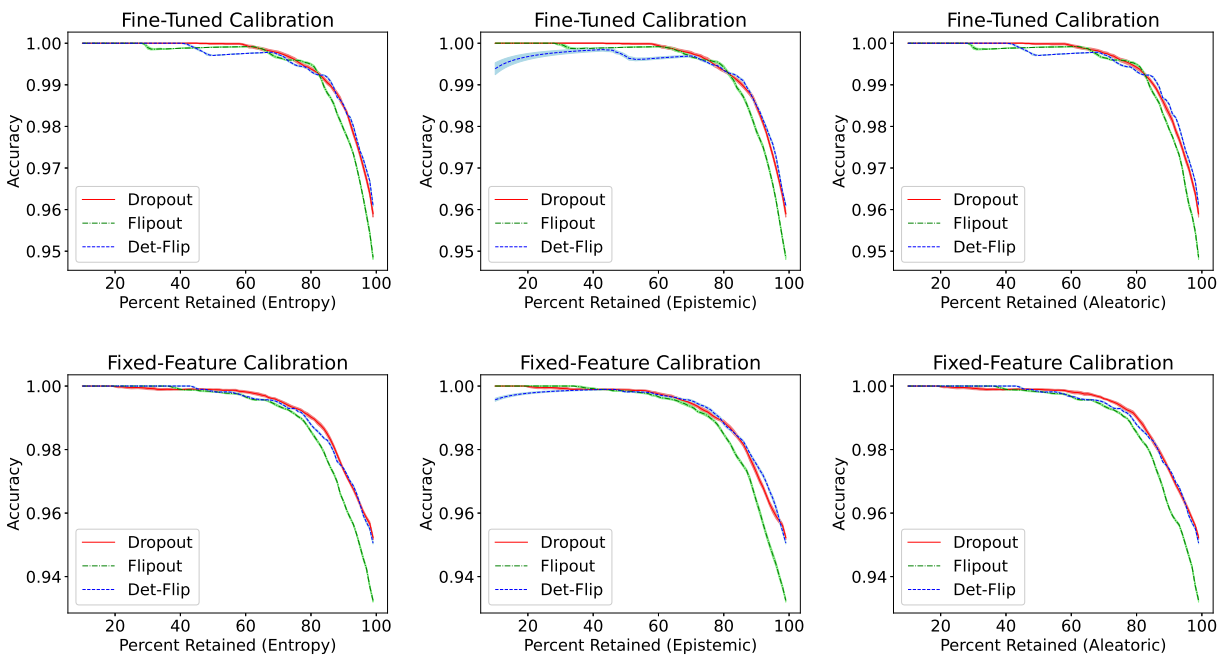


Figure 7: Uncertainty calibration plots comparing Drop, Flip, and Det-Flip VI-PANN variants on ESC-50. Comparison plots of test set accuracy vs. percentage of evaluation data retained based on Entropy (left), Epistemic Uncertainty (center) and Aleatoric Uncertainty (right). Plots corresponding to fine-tuned models are on the top, fixed-feature model plots are on the bottom. Shading represents a 95% CI.

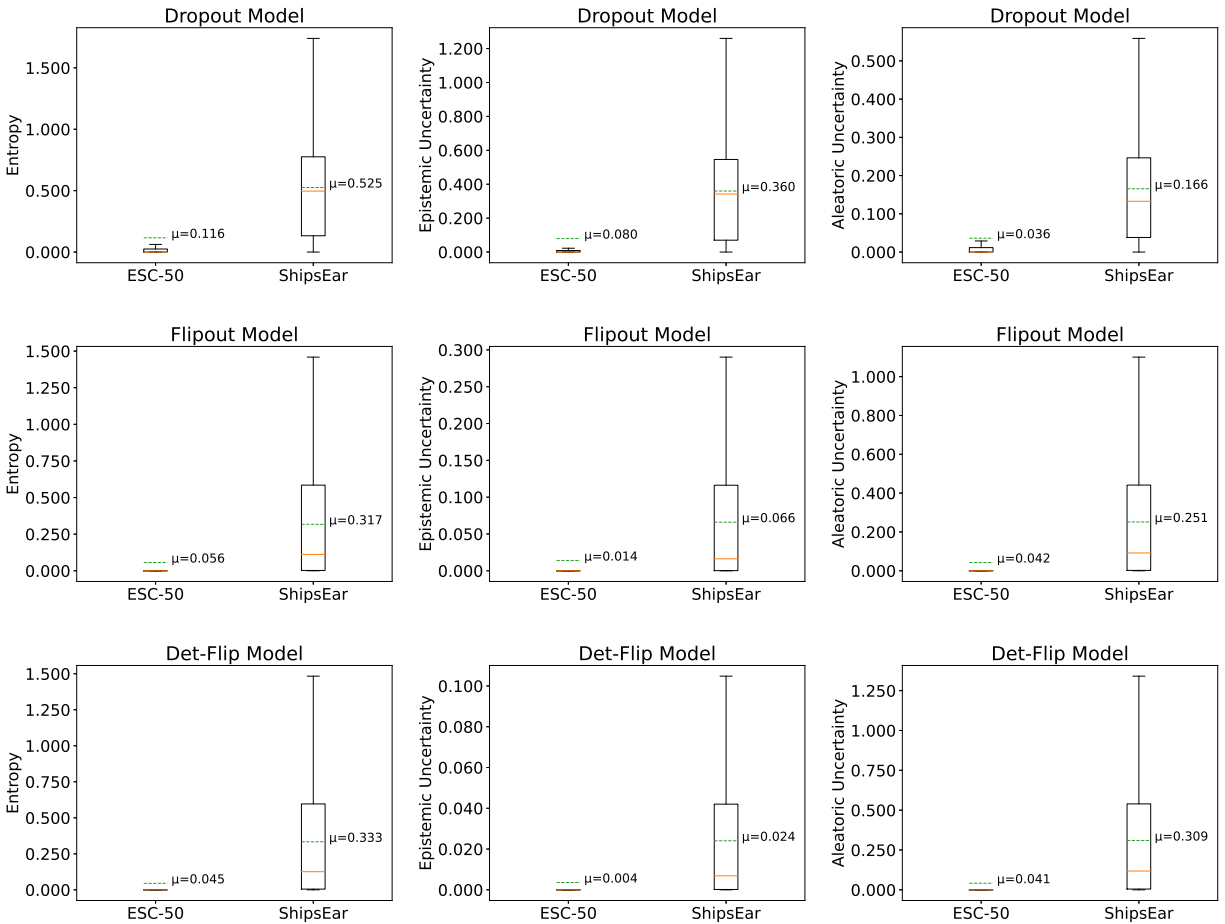


Figure 8: Uncertainty box plots depicting results of MC Dropout (top row), Flipout (middle row), and Det-Flip (bottom row) fine tuned on ESC-50. The plots compare predictive entropy (left), epistemic uncertainty (middle), and aleatoric uncertainty (right) as the models are evaluated on both the ESC-50 and the ShipsEar dataset. Both the median (orange line) and mean (dashed green line) are presented.

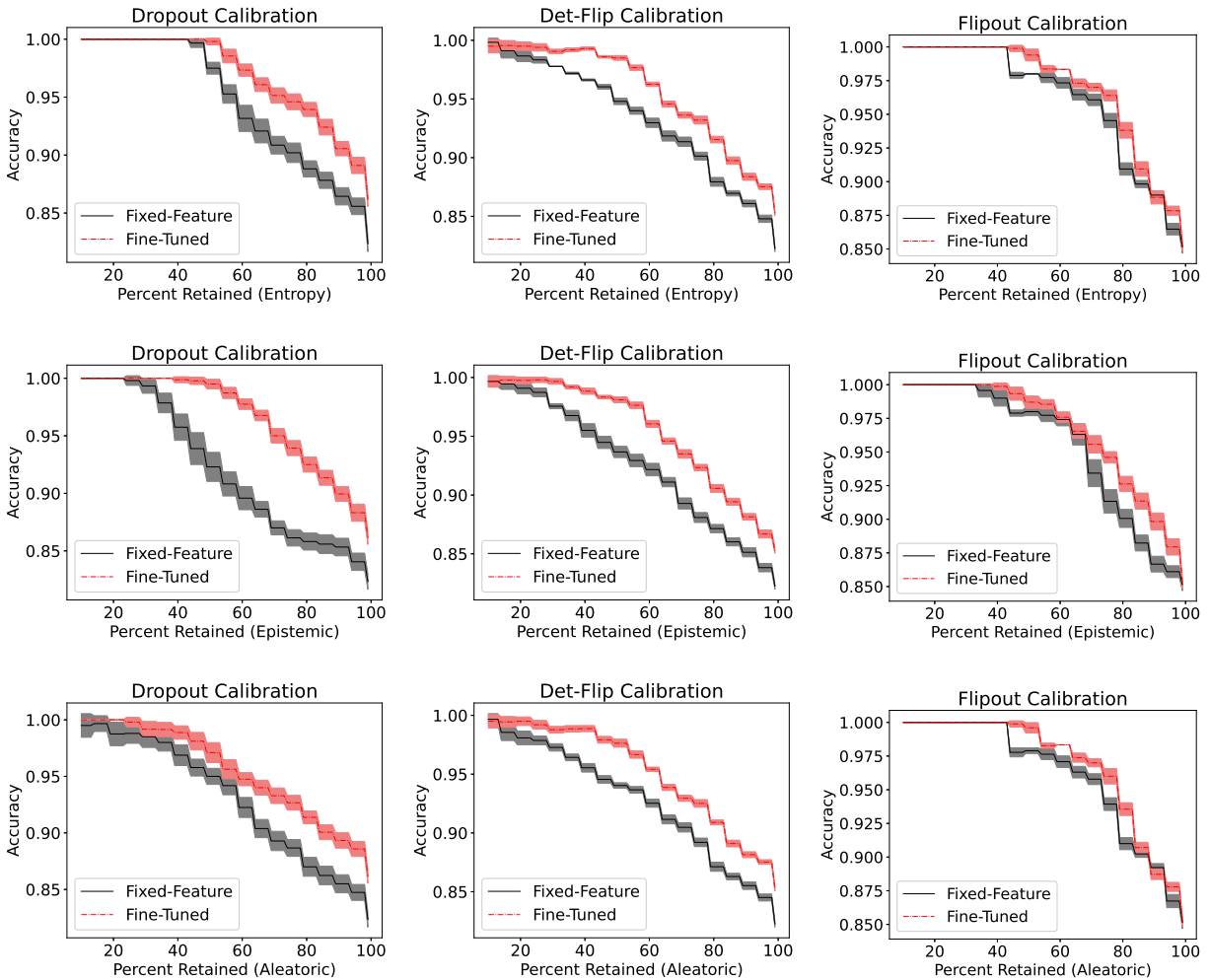


Figure 9: Uncertainty calibration plots comparing fixed-feature and fine-tuning TL techniques on DCASE2013. Comparison plots of test set accuracy vs. percentage of evaluation data retained based on Entropy (top), Epistemic Uncertainty (middle) and Aleatoric Uncertainty (bottom). Drop VI-PANN is on the left, Det-Flip VI-PANN in the center, and Flip VI-PANN on the right. Shading represents a 95% CI.

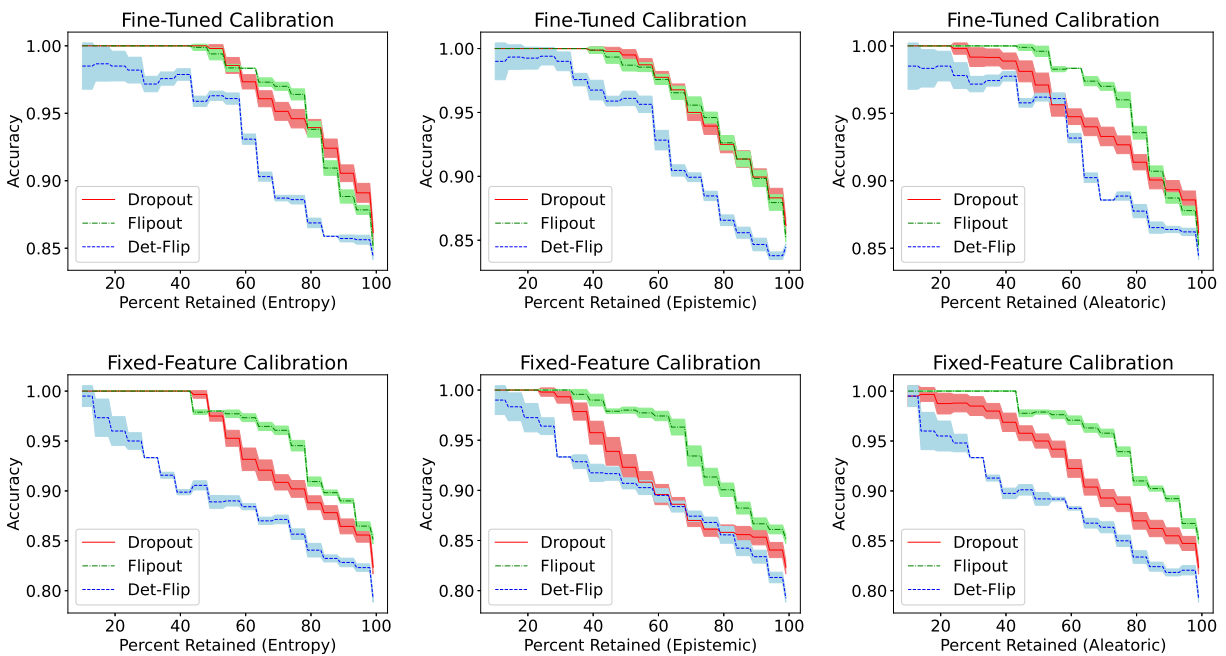


Figure 10: Uncertainty calibration plots comparing Drop, Flip, and Det-Flip VI-PANN variants on DCASE2013. Comparison plots of test set accuracy vs. percentage of evaluation data retained based on Entropy (left), Epistemic Uncertainty (center) and Aleatoric Uncertainty (right). Plots corresponding to fine-tuned models are on the top, fixed-feature model plots are on the bottom. Shading represents a 95% CI.

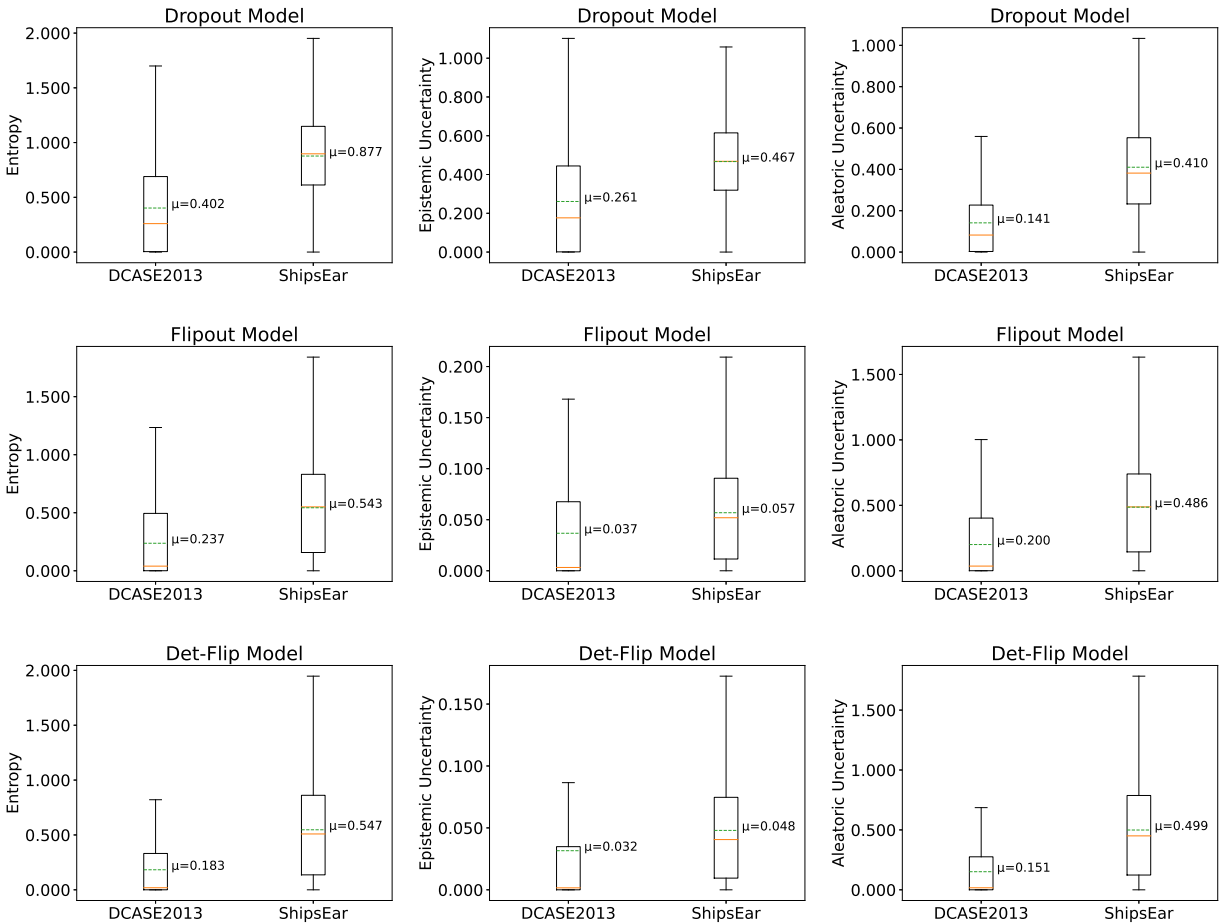


Figure 11: Uncertainty box plots depicting results of MC Dropout (top row), Flipout (middle row), and Det-Flip (bottom row) fine tuned on DCASE2013. The plots compare predictive entropy (left), epistemic uncertainty (middle), and aleatoric uncertainty (right) as the models are evaluated on both DCASE2013 and the ShipsEar dataset. Both the median (orange line) and mean (dashed green line) are presented.